Fluorescence Behavior of Low Molar Mass and Polymer Liquid Crystals in Ordered Solid Films

Brooke M. Conger, John C. Mastrangelo, and Shaw H. Chen*

Materials Science Program, Chemical Engineering Department, and Laboratory for Laser Energetics, Center for Optoelectronics and Imaging, University of Rochester, 240 East River Road, Rochester, New York 14623-1212

Received March 4, 1997; Revised Manuscript Received May 13, 1997[⊗]

ABSTRACT: Fluorescent low-molar-mass and polymeric materials capable of freezing nematic and chiral-nematic liquid-crystalline mesomorphism in a vitreous state were synthesized for the investigation of light absorption, steady-state fluorescence, and decay dynamics via single photon counting, all at room temperature. Monomer (*i.e.*, isolated chromophore) emission was established as the sole decay pathway for singly dispersed chromophores in dilute solution. For chromophores constrained on a cyclohexane ring or a polymethacrylate chain, monomer emission was identified as the predominant decay pathway in dilute solutions. Furthermore, deviation from a single-exponential decay is accompanied by some loss of quantum yield to intramolecular processes. Emission from vitrified films exhibited a red shift of no more than 30 nm and a peak broadening by less than 10 nm compared to dilute solutions of the same compounds. The limited extent of bathochromic shift was considered to have arisen from a microenvironmental effect. The decay dynamics was found to be similar to that in dilute solutions, with a greater loss in quantum yield to both intra- and intermolecular processes existing in solid films. At modest values of order parameter, 0.4−0.6, vitrified nematic and chiral-nematic films produced a fluorescence anisotropy of 0.42 and a dissymmetry factor of 0.25, respectively. The observed degrees of polarization were found to agree fairly well with the theories governing linearly and circularly polarized fluorescence from uniaxially and helically arranged chromophores.

I. Introduction

Optical information processing and display can be accomplished through the use of polarized light. In principle, both passive and active devices can be used to achieve polarization. Aligned materials, such as stretched polymer films containing dichroic dyes, have been successfully implemented as passive devices for linear polarization. In this device concept, light that is polarized along the direction of alignment is absorbed, allowing the light perpendicular to this direction to pass through the material. Circular polarization of light can be achieved using chiral-nematic liquid-crystalline films by taking advantage of the property of selective reflection. In a wavelength region defined by the helical pitch length and the index of refraction, circularly polarized light of one handedness is reflected, allowing light of the other handedness to be transmitted with little or no attenuation. Because of the commercial availability of linear polarizers, linearly polarized light has been extensively investigated for display applications. Circularly polarized light is equally interesting, but it has remained largely unexplored simply because of the lack of readily available devices.

In principle, photonic or electric excitation of films should result in light emission that is linearly and circularly polarized from uniaxially and helically arranged chromophores, respectively. Good alignment of the chromophore is critical to achieving a high degree of polarization. Molecular alignment has been accomplished traditionally by film stretching.[1] In fact, strong linear polarization of both photoluminescence (PL) and electroluminescence (EL) has been reported from films aligned by means of mechanical stretching,[2,3] by vacuum deposition onto a rubbed surface,[4,5] and by way of liquid crystallinity.[6−8] Liquid crystallinity is advantageous in terms of the relative ease with which molecular alignment can be realized across a large area. Both low molar mass nematic fluid and vitrified polymer nematic films have been shown to be capable of polarized PL and EL[6−8] as measured by anisotropy, r, defined as

$$r = \frac{I_{\parallel} - I_{\perp}}{I_{\parallel} + 2I_{\perp}} \tag{1}$$

in which $I_{\parallel}$ and $I_{\perp}$ are the emission intensities observed parallel and perpendicular to the direction of unaxial chromophoric alignment, respectively. In addition, circularly polarized fluorescence (CPF) has been explored using chiral-nematic fluid films[9−14] and polymers with helically arranged pendant groups,[15−17] producing a dissymmetry factor, g_e, as defined below, up to 0.3 and 0.005, respectively:

$$g_e = 2\frac{I_L - I_R}{I_L + I_R} \tag{2}$$

in which I_L and I_R are the intensities of the left- and right-handed circularly polarized emission, respectively. To provide the morphological stability crucial to practical application, we have pursued polarized fluorescence using vitrifiable liquid crystals (VLCs) and polymer LCs functionalized with fluorescent moieties. The source of fluorescence emission will also be elucidated in view of its implication on the extent to which polarization can be achieved.

II. Experimental Section

Synthesis and Characterization of Liquid-Crystalline Materials. The chemical structures and properties of the material systems employed in this work are summarized in Figure 1. Compound **VII** is shown as the precursor to vitrifiable liquid crystal **I**. The fluorescent precursor for vitrifiable LCs **II** and **III** and polymeric LCs **IV**−**VI** is shown

* Author to whom all correspondence should be addressed.
[⊗] Abstract published in *Advance ACS Abstracts,* June 15, 1997.

S0024-9297(97)00291-X CCC: $14.00

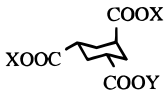

(I) X = Y = R_1
G 60 N 204 I

$R_1 = -(CH_2)_2O-C\equiv C-CN$

(II) X = R_2, Y = R_3
G 68 Ch 277 I; λ_R = 1096 nm

$R_2 = -(CH_2)_3O-CN$

(III) X = Y = R_2
K 132 N 307 I

$R_3 = -(CH_2)_2O-COO-$

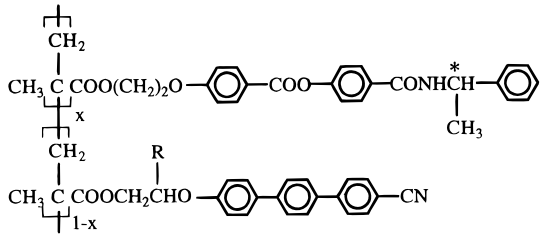

Compound	R	chiral fraction, x	phase transition (°C)	λ_R (nm)	$\overline{M}_w$	$\overline{M}_w/\overline{M}_n$
(IV)	H	0	G 115 N 311 (decomp.)	-	1,900	1.9
(V)	CH_3	0	G 140 N 256 I	-	39,000	2.5
(VI)	CH_3	0.051	G 117 Ch 201 I	1065	15,000	3.4

(VII) $HO(CH_2)_2O-C\equiv C-CN$
K 171 N 238 I

(VIII) $HO(CH_2)_3O-CN$
K 225 N 309 I

Figure 1. Chemical structures and thermotropic properties of low molar mass and polymeric liquid crystals employed in the present study. Symbols: K, crystalline; G, glassy; N, nematic; Ch, cholesteric; I, isotropic.

as **VIII**. The synthesis and characterization of these VLCs and their precursors have been reported previously.[18,19] In what follows, synthetic procedures, using chemicals and reagents all received from Aldrich Chemical Co., will be described for material systems containing cyanoterphenyl as the fluorescent chromophore.

4-Cyanobenzeneboronic Acid. The intermediate 4-cyanobenzeneboronic acid was synthesized according to the procedures reported in the literature.[20] Recrystallization from water provided crystals in 63% yield. NMR (acetone-d_6) spectral data: δ 8.08 (d, aromatic, 2H), 7.80 (d, aromatic, 2H), 7.79 (s, $B(OH)_2$).

4-Hydroxy-4″-cyanoterphenyl. Under a dry nitrogen atmosphere a solution of 2.00 g of 4-cyanobenzeneboronic acid (13.6 mmol) in 10 mL of ethanol was added to a solution of 2.75 g of 4-(4-bromophenyl)phenol (97%, 11.02 mmol) and 0.42 g of tetrakis(triphenylphosphine)palladium(0) (99%, 0.36 mmol) in 20 mL of benzene and 20 mL of aqueous Na_2CO_3 (2 M). The reaction was conducted under reflux until completion in about 4.5 h. The reaction mixture was then shaken with ethyl acetate and brine, and the insolubles were filtered off. The organic layer was dried with anhydrous $MgSO_4$, and the solvent was removed by evaporation *in vacuo*. The crude product was recrystallized from ethanol to produce 1.93 g in 65% yield. NMR (acetone-d_6) spectral data: δ 8.55 (br s, ArOH), 7.95−7.75 (four d, aromatic, 8H), 7.60 (d, aromatic, 2H ortho to cyano), 6.95 (d, aromatic, 2H ortho to hydroxyl).

2-[4-[(4″-Cyanoterphenyl)yl]oxy]ethyl Methacrylate. Under a dry nitrogen atmosphere, 2.07 g of triphenylphosphine (99%; 7.89 mmol) and 2.03 g of 4-hydroxy-4″-cyanoterphenyl (7.49 mmol) were dissolved in 50 mL of anhydrous THF. The solution was chilled in an ice water bath, to which 1.00 g of 2-hydroxyethyl methacrylate (97%; 7.7 mmol) in 20 mL anhydrous THF was added. A solution of 1.38 g of diethyl azodicarboxylate (97%; 7.9 mmol) in 20 mL of anhydrous THF was then added dropwise. The reaction mixture was stirred at room temperature for 24 h. Most THF was then removed by evaporation *in vacuo*, and the residual was shaken with 40 mL of methylene chloride and 40 mL of water. The organic layer was dried with anhydrous Na_2SO_4 before evaporation to dryness. The crude product was purified by flash liquid chromatography using silica gel with methylene chloride as the eluent to produce 1.97 g (69% yield). NMR ($CDCl_3$) spectral data: δ 7.75 (s, aromatic, 4H), 7.70 (s, aromatic, 4H), 7.65 (d, aromatic, 2H ortho to cyano), 7.05 (d, aromatic, 2H ortho to ether), 6.20 (s, alkene, 1H *cis* to ester), 5.65 (s, alkene, 1H *trans* to ester), 4.55 (t, $COOCH_2CH_2$), 4.30 (t, CH_2CH_2OAr), 2.00 (s, CH_3). Elemental anal. Calcd for $C_{25}H_{21}NO_3$: C, 78.31; H, 5.52; N, 3.65. Found: C, 78.00; H, 5.43; N, 3.68.

2-Methyl-2-[(4″-cyanoterphenyl-4-yl)oxy]ethyl Methacrylate. The monomer for the synthesis of a nematic homopolymer, **V**, and a copolymer, **VI**, was prepared by the same procedures as above but using a mixture of hydroxypropyl methacrylate (97%) in place of 2-hydroxyethyl methacrylate. Flash liquid chromatography using silica gel as the eluent produced 2-methyl-2[(4″-cyanoterphenyl-4-yl)oxy]ethyl methacrylate in 47% yield. NMR ($CDCl_3$) spectral data: δ 7.76 (s, aromatic, 4H), 7.68 (s, aromatic, 4H), 7.59 (d, aromatic, 2H ortho to cyano) 7.06 (d, aromatic, 2H ortho to ether), 6.13 (s, alkene, 1H *cis* to ester), 5.59 (s, alkene, 1H *trans* to ester), 4.75 (m, $COOCH_AH_BCH(CH_3)OAr$), 4.40 (dd, $COOCH_AH_BCH$), 4.29 (dd, $COOCH_AH_BCH$), 1.96 (s, alkene, CH_3), 1.44 (d, $CH(CH_3)$). Signals at 4.40 and 4.29 ppm are due to diastereotopic protons that give an AB pattern with a coupling constant of J_{AB} = 21 Hz. Elem anal. Calcd for $C_{25}H_{21}NO_3$: C, 78.57; H, 5.83; N, 3.52. found: C, 78.54; H, 5.79; N, 3.50.

Poly{2(4″-cyanoterphenyl-4-yl)oxy]ethyl methacrylate} (IV). 2[(4″-Cyanoterphenyl-4-yl)oxy]ethyl methacrylate (0.25 g) and 2,2′-azobis(isobutyronitrile) (AIBN) (1 mg) were dissolved in 4 mL of anhydrous THF. Polymerization was conducted at 60 °C under a dry nitrogen atmosphere for 69 h. Presumably because of the limited solubility of the polymer product, white precipitates began to form about 30 min into the polymerization process. The crude product was purified via several dissolution−precipitation cycles. Thermal analysis was performed with differential scanning calorimetry, DSC (Perkin-Elmer DSC-7), at a heating rate of 20 °C/min. The second heating scan produced glass transition temperature, T_g, at 115 °C, beyond which the nematic mesophase was identified with a polarizing optical microscope (Leitz-Orthoplanpol) equipped with a hot stage (FP82, Mettler) and temperature controller (FP80, Mettler). Nematic threaded textures were found to persist up to a decomposition temperature of 311 °C. Polymer molecular weight and its distribution were determined by a GPC system composed of a Constametric metering pump (Milton Roy), two PL gel columns (Hewlett Packard) of 500 and 10 000 Å pore size in series, and a UV−vis differential absorbance detector (V^4, ISCO). With respect to polystyrene standards (Pressure Chemical Co.), it was found that $\bar{M}_w = 1900$ and $\bar{M}_w/\bar{M}_n = 1.9$, where $\bar{M}_w$ and $\bar{M}_w/\bar{M}_n$ are the weight-average molecular weight and polydispersity index, respectively. Elem anal. Calcd for a repeat unit $C_{25}H_{21}NO_3$: C, 78.31; H, 5.52; N, 3.65. Found: C, 77.45; H, 5.50; N, 3.66.

Poly{2-methyl-2-(4″-cyanoterphenyl-4-yl)ethyl methacrylate} (V). 2-Methyl-2-[(4″-cyanoterphenyl-4-yl)oxy]ethyl methacrylate (0.24 g) and AIBN (1 mg) were dissolved in 1 mL of anhydrous THF for polymerization at 60 °C under a dry nitrogen atmosphere for 68 h. In sharp contrast to **IV**, this polymer product remained soluble in THF throughout the entire reaction period, presumably because of the branched spacer inserted between the rigid cyanoterphenyl group and the methacrylate polymer backbone. The product was purified by several dissolution−precipitation cycles. GPC analysis yielded $\bar{M}_w = 39\,000$ and $\bar{M}_w/\bar{M}_n = 2.5$, and DSC analysis gave a T_g at 140 °C followed by a clearing temperature, T_c, at 256 °C where a nematic to isotropic transition occurred. Elem anal. Calcd for a repeat unit $C_{26}H_{23}NO_3$: C, 78.57; H, 5.83; N, 3.52. Found: C, 78.08; H, 5.88; N, 3.57.

Chiral Nematic Copolymer, (VI). 2-Methyl-2-(4″-cyanoterphenyl-4-yl)oxy]ethyl methacrylate (0.17 g), methacrylate-based chiral monomer (0.022 g) containing (*S*)-(−)-1-phenylethylamine, as synthesized previously,[21] and AIBN (1 mg) were all dissolved in 5 mL of anhydrous THF. Copolymerization was conducted at 60 °C under a nitrogen atmosphere for 67 h. The product was purified via dissolution−precipitation cycles. The polymer structure was elucidated with proton-NMR spectroscopy, and the chiral mole fraction was determined by integration of the appropriate NMR signals to be 5.1%. A cholesteric mesophase with selective reflection centered at 1065 nm was identified with hot-stage polarizing optical microscopy between $T_g = 117$ °C and $T_c = 201$ °C, and GPC analysis gave $\bar{M}_w = 15\,000$ and $\bar{M}_w/\bar{M}_n = 3.4$.

Film Preparation. Optical elements were fabricated by sandwiching the material between two fused silica (Esco Products, 1 in. diameter × 1/8 in. thickness, with $n = 1.458$) or calcium fluoride (Optovac, 1 in. diameter × 0.039 in. thickness, with $n = 1.434$) substrates; both were coated with Nylon 66 as an alignment layer. The thickness of the cell was controlled by glass fiber spacers. The devices were heated to 95% of the clearing temperature, sheared to induce alignment, annealed for 3 h, and subsequently cooled at a rate of 30 °C/h to room temperature. For polymer materials with a clearing temperature above 225 °C, the devices were annealed at 220 °C to avoid thermal degradation. Thin films were spin coated from 0.1 to 1 wt % solution in methylene chloride onto substrates with alignment coating. UV−Vis−near-IR absorption and selective reflection measurements were made on a Perkin-Elmer Lambda 9 spectrophotometer. The peaks of interference fringes of the air gap sandwiched between the substrates that were used to calculate the gap thickness were also measured on this instrument. Thickness measurements for single substrate films were accomplished on an interferometer (Zygo New View 100). These measurements were compared to estimations of film thickness from the absorption extinction coefficient measured in dilute solution.

Order Parameter. For nematic liquid-crystalline materials, the order parameter was determined from absorption measurements. The dichroic ratio, *R*, can be measured with various spectroscopic techniques:

$$R = \frac{A_{\parallel}}{A_{\perp}} = \frac{\ln T_{\parallel}}{\ln T_{\perp}} \tag{3}$$

where $T_{\parallel}$ and $T_{\perp}$ are the transmitted intensities of radiation when the electrical field is parallel and perpendicular to the director, respectively. In the present work a Nicolet 20 SXC FTIR spectrometer equipped with a wire grid polarizer was employed for measuring IR polarization of the peak at 2225 cm^{-1} (*i.e.*, stretching of C≡N). The order parameter, *S*, is then determined from *R* according to eq 4:

$$S = \frac{R - 1}{R + 2} \tag{4}$$

The order parameter of the chiral-nematic devices was determined by fitting the experimental selective reflection curve to Good and Karali's theory of light propagation in cholesteric films.[22] The average index of refraction, $\bar{n}$, and the optical birefringence, Δn, were treated as adjustable parameters, with the fitted value of $\bar{n}$ verified against that estimated by a group contribution method.[23] The cholesteric mesophase can be viewed as a stack of nematic layers comprised of cyanoterphenyl groups twisted periodically into a helically arranged supramolecular structure. Based on the optical birefringence and dichroic ratio reported for cyanoterphenyl,[24] the optical birefringence at perfect alignment, Δn_0, was found to be 0.37. The order parameter can be calculated using the relation

$$S = \frac{\Delta n}{\Delta n_0} \tag{5}$$

Fluorescence and Excitation Spectra. Steady-state fluorescence, quantum yield, and polarized fluorescence measurements were made on a spectrofluorimeter (Perkin-Elmer MPF-66). Since measurements of polarization are affected by the angle of excitation or emission, the optical systems as depicted in Figure 2 were implemented to permit straight-through measurement of linearly and circularly polarized fluorescence. The excitation beam is reflected off an aluminum mirror to produce excitation normal to the sample. Background radiation from the excitation beam is filtered using a UG-11 narrow band-pass filter. To minimize optical loss due to reflection, an index matching fluid with $n = 1.500$ (Cargille Laboratories Inc.) is placed between the sample device and the band-pass filter. The excitation wavelengths are 350 nm for polarization measurements and 313 nm for steady-state measurements. Emission peaks were determined on the spectrofluorimeter without polarizers, as the absorption of the polarizers below 400 nm causes a slight shift in the peak. It has been verified that the excitation wavelength has no effect on the shape of the emission spectrum. Excitation spectra were measured on a Spex Fluorolog 2 spectrofluorimeter.

Quantum Yield. Fluorescence quantum yield, η_f, was determined by comparing the integrated photoluminescence with that of a reference with a known quantum yield. For compounds in dilute solution, quinine sulfate (99%; Janssen Chimica) was used as a reference. Quinine sulfate was purified and dried according to Fletcher's procedure.[25] Solutions were prepared in a glovebox under an inert atmosphere to avoid oxygen quenching and were sealed prior to measurement of absorption and fluorescence. The reported η_f value for quinine sulfate at 10^{-3} M in 1.0 N sulfuric acid, 0.546, for 313 nm excitation was employed as the primary reference.[26] This method was validated by measurement of η_f of anthracene (99%; Aldrich Chemical Co.) in ethanol at 10^{-6} M, which was reported to yield $\eta_f = 0.27$.[27] For quantum yield measurements of films, diphenylanthracene (99%; Acros Organics) at 10^{-3} M in PMMA with $\eta_f = 0.83$[27] was employed as the primary

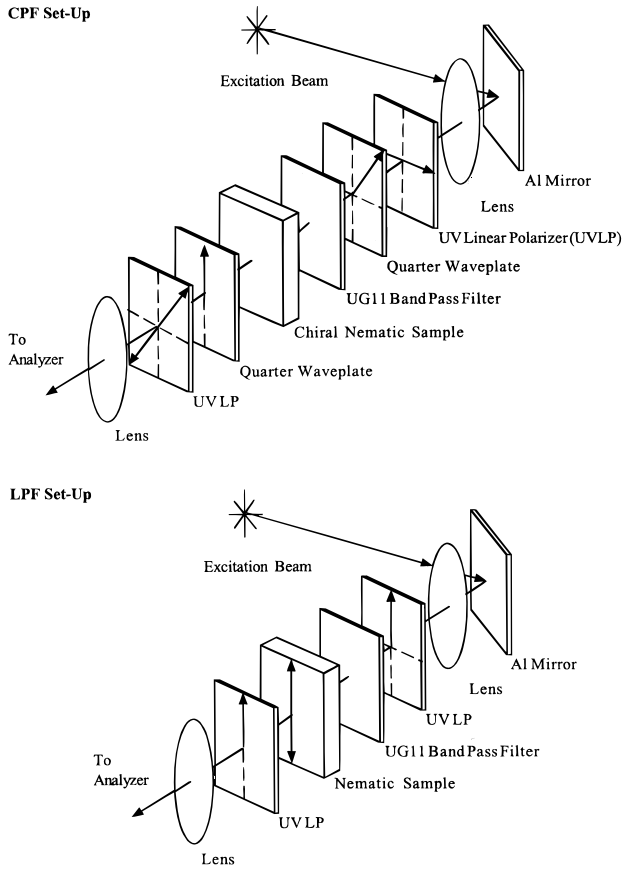

Figure 2. Optical systems inserted in a Perkin-Elmer MPF-66 spectrofluorimeter for the characterization of linearly and circularly polarized fluorescence.

standard. All spectra were collected at room temperature. The equation used in the quantum efficiency calculation is[27]

$$\eta_{f,s} = \eta_{f,r}\left(\frac{I_r^{abs}(\lambda_{ex,r})}{I_s^{abs}(\lambda_{ex,s})}\right)\left(\frac{\bar{n}_s^{\,2}}{\bar{n}_r^{\,2}}\right)\left(\frac{B_s}{B_r}\right) \qquad (7)$$

where the subscripts *r* and *s* denote the reference and sample, respectively, $\bar{n}$ is the average refractive index of the sample to the luminescence, *B* is the integrated area under the corrected emission spectrum, and $I^{abs}(\lambda_{ex})$ is the intensity of absorption at the excitation wavelength, as prescribed by Beer's law. The absorbance at the excitation wavelength was held at a level of 0.1 to ensure experimental accuracy,[28] and the experimental uncertainty was found to be generally within ±5% of the mean of repeated measurements.

Decay Dynamics. Fluorescence decays were recorded via time-correlated single photon counting.[29] The pump laser was a Quantronix 4000 series cw-mode locked Nd:YLF laser with a wavelength of 1053 nm. The frequency-doubled beam was then used to pump a Coherent Series 700 dye laser (Rhodamine 6G), cavity dumper assembly, producing a stream of ca. 6 ps light pulses around the emission maximum of the dye, 570−620 nm. The dye beam was then frequency doubled and filtered to produce an excitation wavelength of 296 nm. Fluorescence was detected at a right angle to the excitation for solutions and a small angle for films by a Hamamatsu R3809U-01 microchannel plate. A Spex 1681 monochromator was used for wavelength selection. Outputs from the photodiode and, after amplification, the microchannel plate led to a Tennelec TC454 constant fraction discriminator, which provided logic start and stop pulses for an Ortec 457 TAC. Output from the TAC led to a Viking Instruments Norland 5000 multichannel analyzer card inside the PC, where Edinburgh Instruments software was used for data acquisition and analysis. The detection rate was ca. 1% of the pulse rate to discriminate between two photon events. A minimum of 10 000 counts was collected in the peak channel.

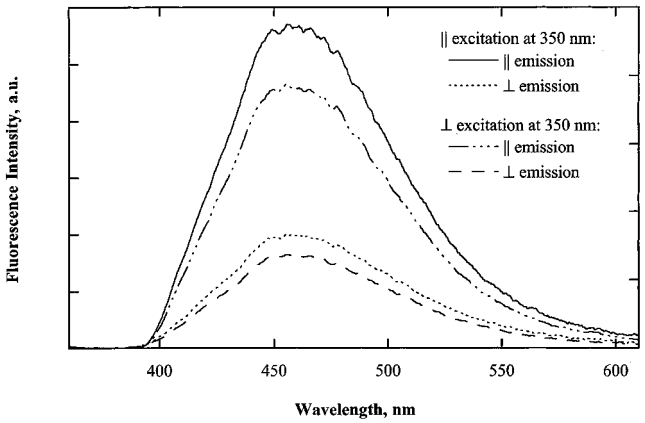

Figure 3. Room-temperature linearly polarized fluorescence from a unaxially aligned solid film 5 μm thick prepared with vitrifiable nematic liquid crystal (**I**).

Table 1. Fluorescence Polarization and Order Parameter for Vitrified Films Prepared with Compounds (I), (II), (IV), and (VI)

compound	film thickness (μm)	r ($\lambda_{excit.}$ = 350 nm)[a]			
		∥ excitation	⊥ excitation	S[c]	S_{em}[e]
I	5	0.38	0.38	0.42	0.43
IV	4	0.46	0.45	0.50	0.50

compound	film thickness (μm)	$-g_e$ ($\lambda_{excit.}$ = 350 nm)[b]			
		RCP excitation	LCP excitation	S[d]	S_{em}[f]
II	18	0.26	0.23	0.54	0.62
VI	18	0.25	0.24	0.46	0.61

[a] r evaluated at $\lambda_{f,max}$ of 455 and 428 nm for **I** and **IV**, respectively. [b] g_e evaluated at $\lambda_{f,max}$ of 427 and 428 nm for **II** and **VI**, respectively. [c] S evaluated with eq 4. [d] S evaluated with eq 5. [e] S_{em} evaluated with eq 39 of ref 30 which relates LPF to order parameter. [f] S_{em} evaluated with the CPF theory reported in ref 30 via minimization of errors between experimentally observed and theoretically predicted g_e values.

III. Results and Discussion

The linearly polarized fluorescence (LPF) spectrum from nematic VLC **I** in the 5 μm film with an *S* of 0.42 is shown in Figure 3. The values of *r* calculated using eq 1 are as presented in Table 1. The fact that the parallel emission intensities are higher than the perpendicular counterparts indicates that the fluorescent chromophores are aligned parallel to the nematic director, resulting in positive *r* values. Note that there is practically no effect on the observed *r* value caused by the polarization state of excitation. Similar behavior was observed for nematic PLC **IV** in the 4 μm film with an *S* of 0.50. The selective reflection spectrum of chiral-nematic VLC **II** in the 18 μm film with an *S* of 0.54 is shown in Figure 4a. The selective reflection wavelength, λ_R, was estimated at 1096 nm with an optical density of 0.27, a value fairly close to 0.30 for perfect alignment. The circularly polarized fluorescence spectrum is shown in Figure 4b, with which g_e was calculated using eq 2. Chiral-nematic PLC **VI** was also fabricated into an 18 μm film with an *S* of 0.46, and its λ_R was found to be 1065 nm. As shown in Table 1, the g_e values of these two chiral-nematic films are practically independent of the polarization state of excitation as well. It should be noted that the absorbance in the spectral region above 400 nm in all four films is negligible. Moreover, in the two chiral-nematic films, fluorescence emission occurs outside the selective reflection band. With (*S*)-(−)-1-phenylethylamine and (−)-5-cholesten-3β-ol as the chiral precursor, chiral-nematic **II** and **VI** possess a left-handed helical supramolecular

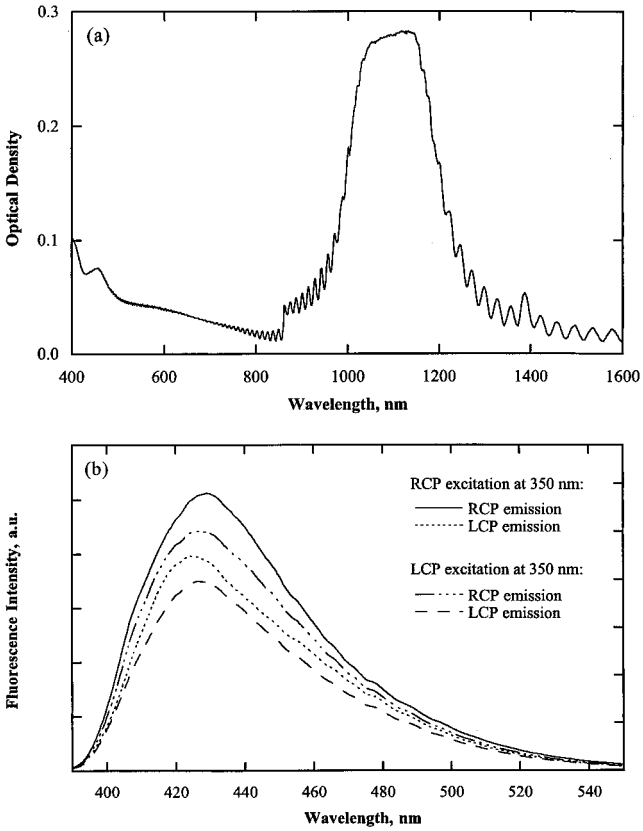

Figure 4. Room-temperature circularly polarized fluorescence from a helically aligned solid film 18 μm thick prepared with vitrifiable chiral-nematic liquid crystal (**II**).

arrangement. As a result, the RCP emission intensities are higher than the LCP counterparts, giving rise to negative g_e values.

The resultant r and g_e values for solid films are quite encouraging in light of the rather modest values of order parameter presently achieved. A recently formulated theory of circularly polarized fluorescence (CPF)[30] is instrumental to the quantification of the effect of helical molecular alignment, as achieved in solid films via chiral-nematic LC mesomorphism, on the degree of polarization. Using $\Delta n_0 = 0.37$ as determined above for use in eq 5, the order parameter based on polarized fluorescence emission, S_{em}, was estimated at 0.62 and 0.61 for compounds **II** and **VI**, respectively, via minimization of variance between the experimental and theoretical g_e values. The discrepancy between the fitted S_{em} values and those determined via selective wavelength reflection, *i.e.*, eq 5, might have originated in the assumption of vanishing optical birefringence made in the CPF theory. In fact, the cyanoterphenyl group is responsible for high optical birefringence value in liquid-crystalline materials.[24] As part of the theoretical development, linearly polarized fluorescence (LPF) was included as eq 39 in ref 30, which governs fluorescence from uniaxially aligned molecules, as realized in solid films via nematic LC mesomorphism. Based on the observed r values, S_{em} was evaluated at 0.43 and 0.50 for compounds **I** and **IV**, respectively. These values are in excellent agreement with those determined via linear dichroism, *i.e.*, eq 4. Better ordered solid films prepared with improved film processing techniques are expected to produce a higher degree of polarization while enjoying the advantages of long-term stability and environmental durability.

To identify the source of emission from vitrified films, the fluorescent behavior of selected VLCs, PLCs, and their fluorescent nematic precursors in dilute solutions was investigated with steady-state and time-resolved spectroscopic techniques. All the fluorescence spectra were single, broad, and structureless peaks with relevant data as summarized in Table 2. In repeated experimentation using **I** as an illustration, the short (τ_1) and long (τ_2) time constants at a given emission wavelength are reproducible to the second and first decimal place, respectively. First, let us look into the nematic groups as isolated molecules, *i.e.*, compounds **VII** and **VIII**, in methylene chloride. Three main observations are noted: (i) The fluorescence spectra of **VII** and **VIII** are independent of concentration from 10^{-6} to 10^{-2} M. (ii) The decay dynamics for both **VII** and **VIII** at a concentration of 10^{-5} M, as monitored by single photon counting, SPC, follows a single-exponential function. (iii) The time constant, $\tau = 1.32$ ns for **VII**, is independent of the emission wavelength chosen for monitoring the decay process ($\lambda_{f,spc}$). The combination of these observations indicates monomer (*i.e.*, isolated chromophore) emission.

It was also found that the normalized fluorescence spectra of VLC and PLC compounds, **I**−**VI**, in dilute solutions are identical to those of their respective precursors, indicating the absence of excimer emission. However, the SPC data of most VLC and PLC compounds follow two-exponential decay functions at a concentration of 10^{-5} M in fluorescent nematic groups, suggesting interchromophoric interaction via an intramolecular process as part of the decay dynamics. The only exception is compound **III**, which showed a single-exponential decay with a time constant very close to that of the precursor, **VIII**. As in the case of **VII** and **VIII**, compound **III** in dilute solution emits light from isolated chromophores. It is expected that the fitted τ_1 and τ_2 values reflect a composite of emissive, energy transfer, and nonradiative processes constituting the overall dynamics. To understand the roles played by these processes, fluorescence quantum yield, η_f, was deter-

Table 2. Fluorescence Behavior of VLCs, PLC, and Their Fluorescent Nematic Precursors in Methylene Chloride

	fluorescence spectra[a]		single photon counting[c,d]		
compound	$\lambda_{f,max}$ (nm)	concn. (M)[b]	$\lambda_{f,spc}$ (nm)	τ (ns)/%	χ^2
I	418	10^{-7}−10^{-2}	400	0.81/84; 8.50/16	1.07
			420	0.81/77; 8.31/23	1.11
			440	0.82/64; 9.31/36	1.10
II	406	10^{-6}−10^{-4}	410		
III	406	10^{-6}−10^{-4}	410	1.66/100	1.23
IV	406	10^{-6}−10^{-4}	410	1.39/57; 3.53/43	1.22
V	406	10^{-6}−10^{-4}	410	1.35/57; 3.37/43	1.15
VI	408	10^{-6}−10^{-4}	410		
VII	416	10^{-6}−10^{-2}	400, 420, 440	1.32/100	1.52 ± 0.09
VIII	408	10^{-6}−10^{-2}	410	1.34/100	1.03

[a] Unpolarized excitation at 313 nm. [b] Concentration expressed in molarity of fluorescent nematic groups, **VII** and **VIII**, in VLCs and PLCs. [c] Unpolarized excitation at 300 nm. [d] All at a sample concentration of 10^{-5} M in fluorescent nematic groups.

Table 3. Fluorescence Behavior of Vitrified Films Prepared with Compounds I, II, and IV−VI

				single photon counting[a]	
compound	film thickness (μm)	$\lambda_{f,max}$ (nm)	$\lambda_{f,spc}$ (nm)	τ (ns)/%	χ^2
I	5	448	430	2.57/57; 8.59/43	1.01
			450	2.63/55; 8.58/45	1.04
			470	2.62/54; 8.57/46	1.08
II	18	419	410	2.53/72; 7.29/28	1.12
			430	2.49/72; 7.27/28	1.09
			450	2.67/69; 7.74/31	1.03
IV	4	426	410	2.25/74; 6.98/26	1.12
			430	2.20/71; 6.76/29	1.01
			450	2.54/75; 8.11/25	1.04
V[b]	0.01	426	410	1.85/79; 6.43/21	1.01
			430	1.89/78; 6.74/22	1.19
			450	2.04/78; 7.46/22	1.19
VI	18	424	410	2.23/82; 7.57/18	1.07
			430	2.24/80; 7.44/20	1.07
			450	2.29/80; 8.06/20	1.09

[a] Unpolarized excitation at 300 nm. [b] Spin-coating, single substrate device.

mined at a concentration of 10^{-5} M. It was found that compounds **VIII**, **III**, and **V** have η_f values of 0.60, 0.56, and 0.49, respectively. Within experimental uncertainty, compound **III** has the same quantum yield as **VIII**, both showing a single-exponential decay as well. However, attaching chromophores onto a polymethacrylate chain incurred some nonradiative loss due most likely to intramolecular processes promoted by the coiled conformation in solution. Therefore, the observed fluorescence from dilute solutions of **I**−**VI** seems to have originated primarily in isolated chromophores because of the absence of fluorescence spectral shift or peak broadening relative to their fluorescent nematic precursors at high dilution. On the other hand, deviation from a single-exponential decay does contribute to some loss of quantum yield.

Let us proceed to examine the fluorescent behavior of ordered, solid films. With the exception of **III**, which was found to recrystallize readily from its vitrified film, **I**−**VI** were all capable of vitrification, producing morphologically stable, ordered films. Compiled in Table 3 are the experimental data collected from steady-state fluorescence and single photon counting. Note that the wavelength of maximum fluorescence intensity, $\lambda_{f,max}$, with polarization control/analysis is red-shifted by 8−10 nm from that without, which can be attributed to light absorption at wavelengths up to 400 nm by the analyzing polarizer used for gathering LPF and CPF spectra. The emission spectra of **I**, **II**, and **IV**−**VI** in solid films showed the same qualitative feature as in dilute solutions, but a red shift in the range from 13 to 30 nm (*i.e.*, ≤0.2 eV) with peak broadening by less than 10 nm (measured as full-width at half-height) was clearly identified, thus precluding excimer emission. However, chromophoric aggregation in the ground state is expected as a result of liquid-crystal alignment and packing at temperatures above T_g from which the mesomorphic order was frozen in the glassy state via slow cooling to room temperature. On the other hand, spin-coated thin films of compounds **I** and **V** on single substrates with a thickness on the order of 0.01 μm gave UV−vis absorption spectra with a red shift at the peak apex of no more than 10 nm compared to dilute solutions. Additionally, the observed value of $\lambda_{f,max}$ was found to be independent of film thickness varied from 0.01 to 5 μm, thus ruling out reabsorption of emission as a reason for the red shift as well. In fact, the minor red shift in $\lambda_{f,max}$ may have arisen from the difference in microenvironment, *viz.*, the oft-quoted solvent effects.[31] This is particularly true in view of the highly polarizable groups present in compounds **I**−**VI** compared to methylene chloride or THF used for solution characterization.

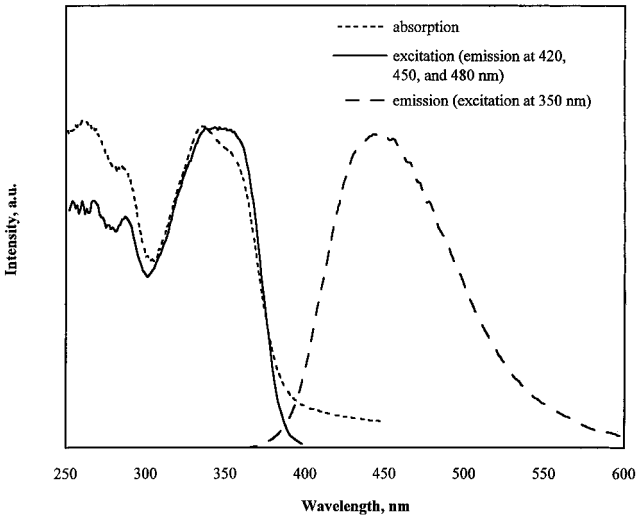

Figure 5. Absorption, excitation, and fluorescence emission spectra, all gathered at room temperature, of a unaxially aligned solid film 0.01 μm thick prepared with vitrifiable nematic liquid crystal (**I**).

The SPC data for vitrified films were found to follow two-exponential decay functions. The relevant data presented in Table 3 indicate that the two time constants and their respective contributions for a given compound are roughly independent of $\lambda_{f,spc}$. To assess the extent of nonradiative loss for lack of clear evidence supporting monomer emission, thin films of **I** and **V** on the order of 0.01 μm in thickness were prepared by spin coating, and their η_f values were evaluated at 0.27 and 0.35, respectively. As a comparison, compounds **I** and **V** yielded an η_f value of 0.51 and 0.49, respectively, at a concentration of 10^{-5} M. Thus, a greater loss in quantum yield was encountered in solid films than in dilute solutions, presumably due both to intra- and intermolecular processes. These solid films were also employed to gather excitation spectra for compounds **I** and **V**, and the results for **I** are presented in Figure 5 as an illustration. It is evident that the excitation spectrum is independent of emission wavelength across the entire fluorescence peak. Furthermore, the excitation spectrum closely follows the absorption spectrum. These two observations, together with the evidence against excimer emission from solid films, lead to the conclusion that absorption and emission of vitrified liquid-crystalline films and dilute solutions involve similar processes. In particular, linearly and circularly

polarized fluorescence, as presented in Figures 3 and 4, originate mainly in emission from isolated chromophores with some nonradiative loss.

IV. Summary

Low molar mass and polymeric systems capable of nematic and chiral-nematic liquid-crystalline mesomorphism were synthesized and characterized for the exploration of polarized fluorescence from ordered solid films. The fluorescent behavior in dilute solution was also examined to furnish new insight into decay pathways as affected by chemical structure and morphology. The main observations emerging from this study are recapitulated as follows:

(1) The characterization of fluorescence in dilute solutions indicates that constraining chromophores on a cyclohexane ring or a methacrylate polymer backbone does not lead to wavelength shift or peak broadening of emission relative to the singly dispersed chromophore. Thus, monomer (*i.e.*, isolated chromophore) is responsible for emission. However, the SPC data for all compounds follow two-exponential functions with the exception of **III** which, along with nematic precursors, follows a single exponential. The deviation from a single-exponential function was found to contribute to some loss in quantum yield via intramolecular processes.

(2) In comparison to dilute solutions, solid films with a frozen liquid-crystalline order gave fluorescence spectra that are red-shifted by 30 nm (or 2 eV) at most with peak broadening by less than 10 nm, suggesting monomer emission. The limited extent of bathochromic shift can be attributed to the microenvironmental effect. As in dilute solutions, the SPC data follow two-exponential functions but with a greater loss in quantum yield to both inter- and intramolecular processes. The excitation spectra of solid films are independent of emission wavelength and closely follow the absorption spectra. Thus, there exists a great deal of similarity in the decay pathways between solid films and dilute solutions.

(3) Solid films comprising uniaxially and helically arranged fluorescent chromophores were prepared with vitrifiable nematic and chiral-nematic liquid crystals, respectively. At modest values of order parameter, $S = 0.4-0.6$, the linear and circular polarization factors, r and g_e, were evaluated at 0.42 and 0.25, respectively. The observed degrees of polarization were also found to be in good agreement with the theories governing linearly and circularly polarized fluorescence with order parameters that assume values consistent with those determined independently by way of linear dichroism and selective wavelength reflection. These are encouraging results and should be amenable to a significant enhancement with an increased order that can be achieved by improved film processing techniques.

Acknowledgment. The authors wish to thank Professor T. Tsutsui of Kyushu University in Japan, Dr. A. Schmid of the Laboratory for Laser Energetics (LLE), and Professor S. A. Jenekhe and Dr. L. Lin, both at the University of Rochester, for their advice and helpful discussions. They also thank Dr. S. D. Jacobs of LLE for his suggestion of the optical setup depicted in Figure 2 for the characterization of LPF and CPF. This research was supported by U.S. National Science Foundation under Grant CTS-9500737 and the Japanese Ministry of International Trade and Industry. Part of this work was also supported by the U.S. Department of Energy Office of Inertial Confinement Fusion under Cooperative Agreement No. DE-FC03-92SF19460, the University of Rochester, and the New York State Energy Research and Development Authority. The single photon counting experiment and interferometric measurement of film thickness were performed using the facilities available at the NSF Center for Photoinduced Charge Transfer and the Center for Optics Manufacturing, both at the University of Rochester.

References and Notes

(1) Dirix, Y.; Tervoort, T. A.; Bastiaansen, C. *Macromolecules* **1995**, *28*, 486.
(2) Hagler, T. W.; Pakbaz, K.; Voss, K. F.; Heeger, A. J. *Phys. Rev. B* **1991**, *44*, 8652.
(3) Dyreklev, P.; Berggren, M.; Inganäs, O.; Andersson, M.; Wennerström, O.; Hjertberg, T. *Adv. Mater.* **1995**, *7*, 43.
(4) Era, M.; Tsutsui, T.; Saito, S. *Appl. Phys. Lett.* **1995**, *67*, 2436.
(5) Marks, R. N.; Biscarini, F.; Zamboni, R.; Taliani, C. *Europhys. Lett.* **1995**, *32*, 523.
(6) Sariciftci, N. S.; Lemmer, U.; Vacar, D.; Heeger, A. J.; Janssen, R. A. J. *Adv. Mater.* **1996**, *8*, 651.
(7) Lüssem, G.; Festag, R.; Greiner, A.; Schmidt, C.; Unterlechner, C.; Heitz, W.; Wendorff, J. H.; Hopmeier, M.; Feldmann, J. *Adv. Mater.* **1995**, *7*, 923.
(8) Lüssem, G.; Geffarth, F.; Greiner, A.; Heitz, W.; Hopmeier, M.; Oberski, M.; Unterlechner, C.; Wendorff, J. H. *Liq. Cryst.* **1996**, *21*, 903.
(9) Sisido, M.; Wang, X.; Kawaguchi, K.; Imanishi, Y. *J. Phys. Chem.* **1988**, *92*, 4801.
(10) Kawaguchi, K.; Sisido, M.; Imanishi, Y. *J. Phys. Chem.* **1988**, *92*, 4806.
(11) Sisido, M.; Takeuchi, K.; Imanishi, Y. *J. Phys. Chem.* **1984**, *88*, 2893.
(12) Sisido, M.; Takeuchi, K.; Imanishi, Y. *Chem. Lett.* **1983**, 961.
(13) Stegemeyer, H.; Stille, W.; Pollmann, P. *Isr. J. Chem.* **1979**, *18*, 312.
(14) Pollmann, P.; Mainusch, K. J.; Stegemeyer, H. *Z. Phys. Chem.* **1976**, *103*, 295.
(15) Schlessinger, J.; Steinberg, I. Z. *Proc. Natl. Acad. Sci. USA* **1972**, *69*, 769.
(16) Sisido, M.; Egusa, S.; Okamoto, A.; Imanishi, Y. *J. Am. Chem. Soc.* **1983**, *105*, 3351.
(17) Langeveld-Voss, B. M. W.; Janssen, R. A. J.; Christiaans, M. P. T.; Meskers, S. C. J.; Dekkers, H. P. J. M.; Meijer, E. W. *J. Am. Chem. Soc.* **1996**, *118*, 4908.
(18) Shi, H.; Chen, S. H. *Liq. Cryst.* **1995**, *18*, 733; **1995**, *19*, 785.
(19) Chen, S. H.; Mastrangelo, J. C.; Blanton, T. N.; Bashir-Hashemi, A. *Liq. Cryst.* **1996**, *21*, 683.
(20) Hird, M.; Toyne, K. J.; Gray, G. W.; Day, S. E.; McDonnel, D. G. *Liq. Cryst.* **1993**, *15*, 122.
(21) Krishnamurthy, S.; Chen, S. H. *Macromolecules* **1991**, *24*, 3481.
(22) Good, R. H., Jr.; Karali, A. *J. Opt. Soc. Am. A* **1994**, *11*, 2145−2155.
(23) Van Krevelen, D. W. *Properties of Polymers: Their Estimation and Correlation with Chemical Structures*; Elsevier Scientific Publishing Company: New York, 1976; Chapter 10.
(24) Wu, S.-T.; Ramos, E. *J. Appl. Phys.* **1990**, *68*, 78−95.
(25) Fletcher, A. N. *Photochem. Photobiol.* **1969**, *9*, 439.
(26) Melhuish, W. H. *J. Phys. Chem.* **1961**, *65*, 229.
(27) Demas, J. N.; Crosby, G. A. *J. Phys. Chem.* **1971**, *75*, 991.
(28) Guilbault, G. G. In *Practical Fluorescence*; Guilbault, G. G., Ed.; Marcel Dekker: New York, 1990; Chapter 1.
(29) O'Connor, D. V.; Phillips, D. *Time-correlated Single Photon Counting*; Academic Press: New York, 1984.
(30) Shi, H.; Conger, B. M.; Katsis, D.; Chen, S. H. *Liq. Cryst.*, in press.
(31) Lakowicz, J. R. *Principles of Fluorescence Spectroscopy*; Plenum Press: New York, 1983; Chapter 7.

MA9702915